Molecular Catalysis 439 (2017) 163–170

Contents lists available at ScienceDirect

Molecular Catalysis

journal homepage: www.elsevier.com/locate/mcat

MCAT

Editor's choice paper

Theoretical and experimental study of ethanol adsorption and dissociation on β-Mo_2C surfaces

Nilda Chasvin[a], Alejandra Diez[a], Estela Pronsato[b], Romana Šedivá[c], Viktor Johánek[c], María Alicia Volpe[d,*], Carolina Pistonesi[b]

[a] Departamento de Química, Universidad Nacional del Sur, & INQUISUR(UNS-CONICET), Av. Alem 1253, 8000 Bahía Blanca, Argentina
[b] Instituto de Física del Sur IFISUR, Departamento de Física, Universidad Nacional del Sur, (UNS)-CONICET, Av. Alem 1253, 8000 Bahía Blanca, Argentina
[c] Department of Surface and Plasma Science, Charles University, Prague, Czech Republic
[d] Planta Piloto de Ingeniería Química, UNS-CONICET, Camino Carrindanga Km 7, 8000 Bahía Blanca, Argentina

ARTICLE INFO

Article history:
Received 3 March 2017
Received in revised form 30 June 2017
Accepted 3 July 2017
Available online 16 July 2017

Keywords:
Molybdenum carbide
Self-consistent DFT
Ethanol dissociation
Nudged elastic band method

ABSTRACT

The adsorption and dissociation of ethanol over molybdenum carbide were studied in the context of the production of H_2 from alcohols. A β-Mo_2C catalyst was prepared from char and Mo salts. The sample was characterized by N_2 sorptometry at 77 K, temperature programmed reaction of H_2, X-ray diffraction (applying Rietveld approximation) and X-ray photoelectron spectroscopy for investigating on the catalytic properties of the prepared sample. The catalyst would be active and stable for H_2 dissociation at 500–600 K. The value of ethanol adsorption energy was −0.92 eV, as calculated on β-Mo_2C (001) surface by means of self-consistent density functional calculations. A transfer of electron density from the surface to adsorbed ethanol was concluded from calculations. Plausible reaction pathways corresponding to ethanol dissociation to ethoxy were theoretically studied by using the Climbing Image Nudged Elastic Band (CI-NEB), which shows and activation energy value of 0.57 eV.

1. Introduction

Alcohols decomposition on heterogeneous catalysts is an important reaction related to H_2 production for fuel cell [1–3]. Pt supported on Al_2O_3 is active for this reaction, however this catalyst produces CO and it becomes easily deactivated [4,5]. Taking into account the technological importance of alcohols decomposition, there exists a great interest to find new catalysts, more efficient, and more stable under reaction conditions than traditional Pt based ones.

Transition metal carbides have been studied as catalysts for different reactions because of their low price and peculiar chemical and physical properties. Levy and Boudart have concluded that tungsten carbide (WC) exhibits similar or even better catalytic behaviour than Pt for several reactions [4]. Later, other works have demonstrated that molybdenum carbide (Mo_2C) is effective for carrying out different reactions, as for example alcohols decomposition [6–9] and CH_4 aromatization [10]. Mo_2C exists in different crystalline phases such as cubic γ-Mo_2C, hexagonal α-Mo_2C, δ-Mo_2C and orthorhombic β-Mo_2C (following Joint Committee on Power Diffraction Pattern). Although in earlier works, the hexagonal α phase was considered to be the active one for alcohols dissociation, at the present, β-Mo_2C is considered to be responsible for developing activity [1].

Theoretical studies, at density functional theory level, focused on the catalytic activity of Mo_2C. Ren et al. have studied the adsorption of O_2, H, CH_2 and C_2H_2 on Mo_2C surfaces, finding stronger adsorptions on the Mo-terminated than on the C-terminated surfaces [11,12]. Water-gas shift reaction over β-Mo_2C(001) surfaces has been studied by Tominaga and Nagai finding a reaction pathway for CO_2 formation [13], they also have analyzed methane reforming on the same surface, modeling the formation of ethylene or ethane [14]. Some of us have obtained theoretical results on CO adsorption [15,16] and also on the dissociation of methyl iodide [17] and methanol [2,18] on β-Mo_2C(001) surface, finding adsorption energies, vibrational frequencies and reaction pathways in agreement with experimental values.

In the present work, the study of the adsorption and the dissociation of ethanol on a β-Mo_2C catalyst is carried out from two different approaches, a theoretical and an experimental one. A model β-Mo_2C catalysts is studied with self-consistent density functional theory (DFT) calculations, to carry out the analysis of the

* Corresponding author.
E-mail address: mvolpe@plapiqui.edu.ar (M.A. Volpe).

http://dx.doi.org/10.1016/j.mcat.2017.07.003
2468-8231/

adsorption and the subsequent dissociation of ethanol. In addition, reaction pathways for the ethanol dissociation on molybdenum carbide were analyzed by using the climbing image nudged elastic band method (CI-NEB). Besides, a β-Mo_2C sample is prepared from commercial carbon and molybdenum salts. The sample is characterized with N_2 sortometry, temperature programmed reaction of H_2, X-ray diffraction (performing a Rietveld refinement) and X-ray photoelectron spectroscopy. An attempt to conclude about the catalytic properties of molybdenum carbide for the ethanol decomposition for producing H_2 is carried out.

2. Methods and materials

2.1. Catalyst preparation and characterization

Mo_2C was prepared from Molybdic acid (Sigma, 98.98%), ammonium molybdate (Sigma, 98.98%), and char (Anedra). 0.22 g of molybdic acid, 0.23 g of ammonium salt and 0.55 g of char were put in a furnace under H_2 flow (5 ml/min) at 650 °C, for 4 h. Finally the material was cooled down to room temperature under H_2 flow, subsequently the H_2 flow was switched to a N_2 flow. The resulting material was characterized by X-ray diffraction (XRD) in a Philips PW1710 BASED instrument with CuKα radiation, within a 2θ range of 20–110°, with a scanning speed of 1.2°/min. The pattern was analysed following Rietveld approximation. Textural characterization of the catalysts was carried out by N_2 adsorption at 77 K in a Quantachrom Nova 1200e sorptometer. The specific surface areas were calculated employing the BET equation and the pore volume by the Dubinin–Radushkevich equation.

Ethanol decomposition process was monitored by temperature programmed reaction (TPRx). Experiments were conducted in a custom-built laboratory micro-reactor system. The sample is sandwiched between a resistive heater at the bottom and a silicate glass with two feeding holes and a network of channels for effective gas distribution over the sample surface at the top, forming a small micro-reactor cell volume. Silicon rubber sealing (100 mm thick) is placed around the perimeter of the sample to prevent leakage. The reactor cell is incorporated in a massive metal block with integrated thermocouple (K-type) to assure good thermal stability and spatial homogeneity. All experiments were done at total gas pressure of 1 bar and the sample temperature ranging between 300 and 630 K; the heating rate of the temperature ramps was set to 2 K/min. Ethanol was fed to the reactor in the form of vapor generated by bubbling pure helium (Linde Gas, 4.6, 20 sccm flow rate) through a heated saturator (303 K) filled with liquid ethanol (Penta, 99.5% purity). The He flow was adjusted precisely by Alicat Scientific mass flow controller. All stainless-steel tubing between the saturator and the reaction cell was heated to about 360 K to prevent condensation of ethanol vapor before reaching the sample. The stream of products leaving tinly unreacted ethanol vapor and water) from clogging the metering valve or deteriorating vacuum in the QMS chamber.

The sample was also characterized by X-ray photoelectron spectroscopy (XPS). The sample was previously calcined at different temperatures (250, 400 and 600 °C) *ex-situ*. Another pre-treatment consisted of heating at 250, 400, 600 and 800 °C in the apparatus chamber. For all the cases, binding energy, BE, of $Mo3d_{5/2}$ were measured following charge correction employing C1s peak.

2.2. Computational method and surface model

The density functional theory, implemented by the Vienna *ab initio* simulation package (VASP) [19], which employs a plane-wave basis set and a periodic supercell method [20,21] was applied for studying β-Mo_2C. Potentials within the projector augmented wave method (PAW) [22] and the generalized gradient approximation (GGA) with the Perdew–Burke–Ernzerhof (PBE) functional were used [23,24].

For bulk optimization, the lattice parameters for β-Mo_2C were obtained by minimizing the total energy of the unit cell using a conjugated gradient algorithm to relax the ions and considering a set of $7 \times 7 \times 7$ Monkhorst–Pack k-points to sample the Brillouin Zone [25].

Molybdenum terminated and carbon terminated (001) surfaces were modeled with slabs of five layer thicknesses using the DFT lattice parameters, previously obtained from bulk optimization. During optimization the first two layers were allowed to relax, and a set of $3 \times 3 \times 1$ Monkhorst-Pack k-points was used.

The adsorption of the ethanol molecule was investigated on different sites of Mo and C terminated surfaces, with ethanol coordinated *via* the O atom to the substrate. For these calculations, the adsorbed species and the first two surface layers were allowed to relax. A kinetic energy cutoff of 750 eV was employed for all the calculations. Also, for all the geometry optimizations a cut condition of 10^{-3} eV for the total energy of the system between two ionic relaxation steps, was considered. The electronic relaxation convergence criterion was set to 10^{-4} eV. Van der Waals interaction between pairs was included by means of Grimme DFT-D2 method [26].

The ethanol adsorption energy was computed by subtracting the energies of the gas-phase species and the surface from the energy of the adsorbed system as follows:

$$E_{ads}(\text{ethanol}) = E(\text{ethanol/slab}) - E(\text{ethanol}_{gas}) - E(\text{slab})$$

With this definition, negative adsorption energies correspond to energetically favorable adsorption sites on the surface. The more negative the values, the stronger the adsorption bonds.

Ethanol dissociation to ethoxy on both Mo and C terminated surfaces was also investigated. Plausible reaction pathways were modeled using the climbing image nudged elastic band method (CI-NEB) [27]. Eight geometry images for each cycle were considered. The nature of the transition states on the potential energy surface has been tested based on the analysis proposed by Henkelman et al. [28] and its configuration was verified by a vibrational analysis, finding one imaginary frequency.

The electronic charges on atoms were computed using Bader analysis [29]. The net charge of the ethanol/ethoxy molecule was calculated adding the individual charges of the C, H and O atoms.

3. Results and discussion

3.1. Experimental characterization

The Mo_2C sample prepared form molybdenum salts and char was analysed by XRD to confirm the presence of β-phase. The XRD pattern of the sample is shown in Fig. 1, in which the experimental data, as well as the ones calculated from the Rietveld method approximation are shown. The presence of other species than molybdenum carbide could be disregarded since no other peaks than the corresponding to the β-Mo_2C phase was detected. Besides, the position of the diffraction peaks is in line with the β-Mo_2C phase crystalline structure, which has an orthorhombic crystal structure with Mo atoms slightly distorted from their positions in closed-packed planes and carbon atoms occupying one-half of the octahedral interstitial sites.

The agreement between experiment and calculation following Rietveld method is quite high for the low angle diffraction peak. On the other hand, at high 2θ angles, the agreement is rather low. The disagreement would be more likely associated to an instrumental artifact, originated in the fixed slit of the diffractometer.

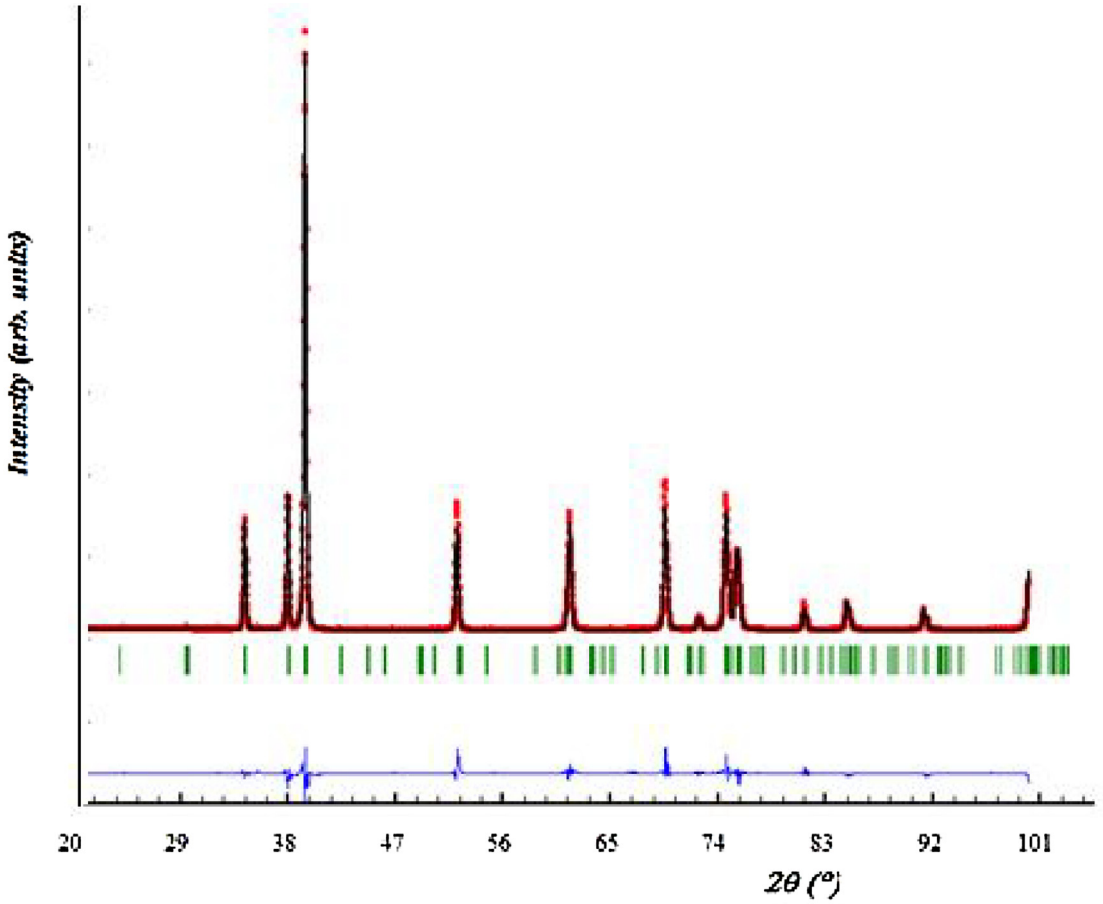

Fig. 1. XRD of Mo_2C. (▪) experimental data, (—) Rietveld calculation, (|||) Bragg position, (___) experimental/theoretical differences.

Table 1
Crystallographic parameters and atomic positions corresponding to Mo_2C sample prepared from carbon and molybdenum salts.

Phase	β-Mo_2C
Crystal System	orthorhombic
Space group	*Pbcn*
a(Å)	4.73373
b(Å)	6.02935
c(Å)	5.20613
V(Å^3)	148.5895
Size crystal (nm)	42.37

Site	Atom.	x	y	z	$W_{Position}$
Mo	Mo^{+2}	0.24617	0.12796	0.07926	8d
C	C^{-4}	0.00000	0.38546	0.25000	4c

Thus, from the analysis of XRD results, it is concluded that the sample corresponds to β-Mo_2C phase.

The crystallographic parameters are reported in Table 1. These values are quite similar to the ones obtained by Parthé et al. (a = 4.725 Å, b = 6.022 Å, c = 5.195 Å) from a neutron diffraction study [30].

The specific surface area of the molybdenum carbide sample (calculated from BET approximation) was 34 m^2/g, while the pore volume was 0.03 cm^3/g. Both values remained constant following a calcination treatment at 673 K, indicating that the sample is relatively stable. We will revert to this matter latter, following the analysis of XPS characterization.

Fig. 2a shows Mo 3d XP peaks of the β-Mo_2C sample submitted to a calcination treatment at different temperatures. In Table 2, BE values of Mo $3d_{5/2}$ transitions, corresponding to the different temperatures are reported.

Table 2
Binding Energies (BE) of $3d_{5/2}$ XP peaks corresponding to the prepared β-Mo_2C catalyst submitted to calcination and to heating at the 298–1073 K.

Treatment temp. (K)	BE Mo$3d_{5/2}$ calcination (eV)	BE Mo$3d_{5/2}$ heating. (eV)
298	232.5	232.5
523	232.3	232.0
673	232.7	229.3
873	234.3	228.0
1073	—	227.6

For the non-treated sample the BE of $3d_{5/2}$ corresponds to molybdenum carbide [9]. For calcination temperatures in the 473–673 K range, BE slightly increases, showing that the catalyst is

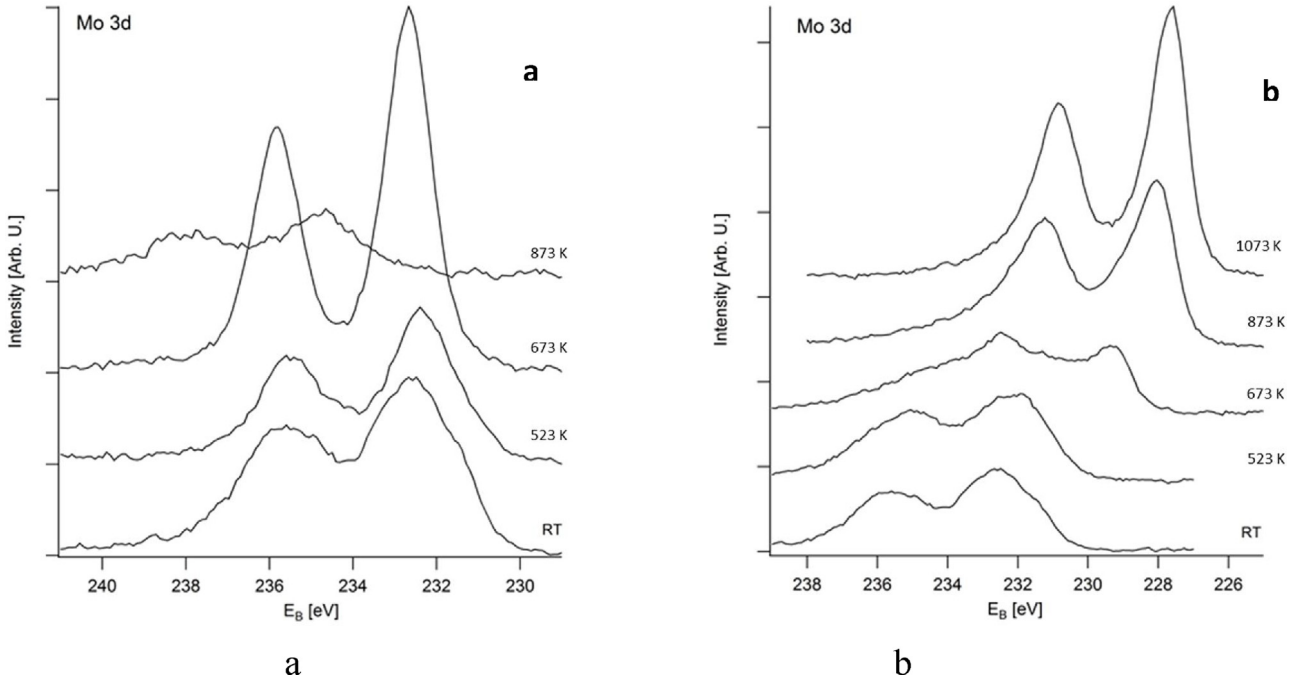

Fig. 2. Mo XP 3d peaks of Mo_2C catalyst submitted to calcination (a); and to heating under UHV conditions (b).

chemically stable in this range of temperatures. On the other hand, at 873 K, a strong diminution of the intensity of the peaks as well as an important shift in BE values were observed. Both phenomena would be related with the volatilization of MoO_3. The volatilization of MO_3, above 700 °C under oxidizing conditions, is a well documented phenomenon which would be the origin of the diminution of molybdenum XP peaks [31]. It could be concluded that the catalyst is quite stable, since up to 673 K molybdenum carbide is not decomposed, which is in line with the stability of specific surface area determined by N_2 sorptometry. This is an important property of the catalyst that indicates that a regeneration of spent molybdenum carbide catalysts by calcination treatment could recover the original catalytic properties.

For the case of the catalyst heated under ultra-high vacuum conditions in the apparatus chamber, at temperature of 673 K a notable shift of BE towards lower values was observed. This shift would be ascribed to the formation of Mo^0. In addition, an increase in the intensity of the peaks is detected probably associated with the surface enrichment with reduced molybdenum.

Summing up, from the analysis of XPS results it could be concluded that the Mo_2C catalyst would be quite stable for reaction and or regeneration temperatures up to 673 K.

Regarding TPRx characterization, the results corresponding to desorption of H_2 (mass 4 a.m.u.) are shown in Fig. 3. It is observed that the signal starts to increase at approximately 500 K, reaching a maximum at 600 K. From these results it could be suggested that the working temperature of the catalyst would be in the 500–600 K range, which would not lead to the carbide decomposition, following the above commented XPS results.

3.2. Theoretical calculations

The β-Mo_2C phase has an orthorhombic crystal structure with Mo atoms slightly distorted from their positions in close-packed planes and carbon atoms occupying one-half of the octahedral interstitial sites. The corresponding unit cell is composed by eight molybdenum atoms and four carbon atoms.

The lattice parameters for the β-Mo_2C catalyst were calculated by DFT, giving rise to the following values: a = 4.76 Å, b = 6.08 Å, and c = 5.23 Å, which are very close to the above reported experimental values obtained from XRD characterization (see Table 1).

Formation energy of molybdenum carbide (E_f) was calculated from the relaxed bulk energy (E_{bulk}) and the energy of molybdenum in a face-centered cubic crystal structure (E_{Mo}) and that of carbon in graphite structure (E_C) according to the following equation

$$E_f = -\frac{(n_{Mo}E_{Mo} + n_C E_C) - E_{bulk}}{n_{Mo} + n_C}$$

Where n_{Mo} and n_C denotes the number of atoms of the specified element on the unit cell. Our computed value of the formation energy is 0.45 eV, very close to the experimental value of 0.49 eV [32].

The structure of the β-Mo_2C (001) surface includes a series of alternating Mo and C layers. Two surfaces, molybdenum-terminated and carbon-terminated, with slabs of 6.08 Å by 10.46 Å and five layer thickness were modeled. The vacuum spacing between two repeated slabs was 15.23 Å. During the optimization the first two layers were allowed to relax. Fig. 4 shows the supercell corresponding to the Mo-terminated surface (a similar one corresponds to the C-terminated one).

Ethanol adsorption was analyzed on several adsorption sites on the Mo- and C- terminated surfaces (see Fig. 4). Table 3 shows the calculated adsorption energies and selected equilibrium distances and angles for the lowest energy adsorption sites. According to calculations, the ethanol molecule preferentially adsorbs on Mo top sites on the β-Mo_2C (001) surface. The lowest energy configuration for both surfaces corresponds to a Mo top site, with an adsorption energy value of −0.92 eV on Mo- terminated surface, and a value of −0.43 eV on C-terminated surface. The former value is in good agreement with TPD experimental value of −0.89 eV for the chemisorption of ethanol [33].

Fig. 5a and b show schematic views of ethanol adsorbed on a Mo top site on a Mo-terminated surface and on a Mo-top site on a C-terminated surface, respectively. For both cases, molecular C—C bond is oriented almost parallel to the surface.

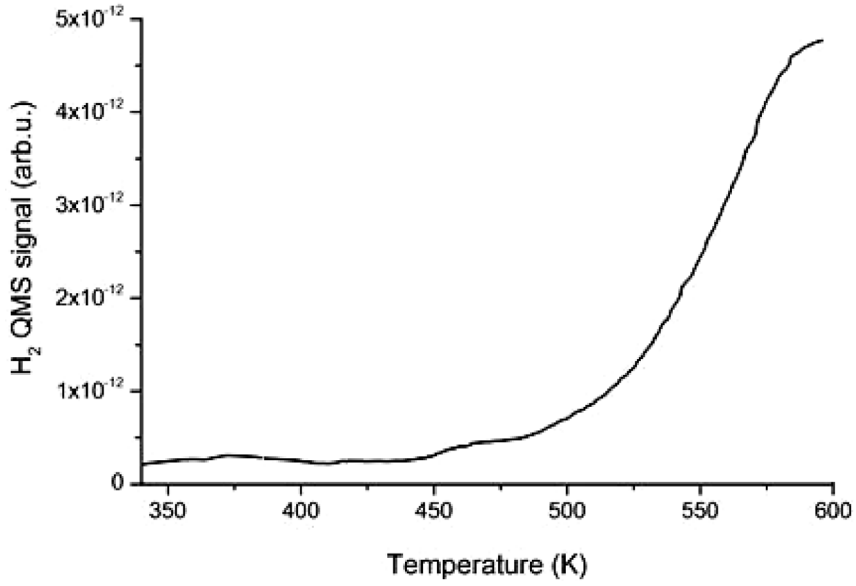

Fig. 3. TPRx profile corresponding to the desorption of H_2 on β-Mo_2C.

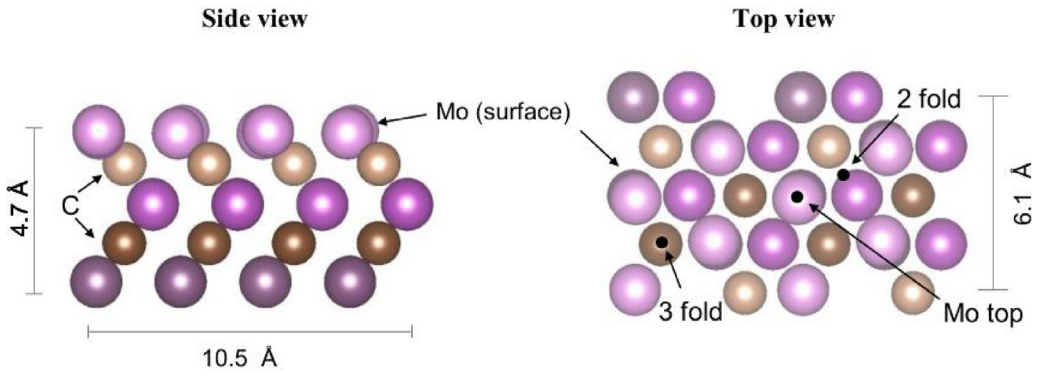

Fig. 4. Two views of the Mo-terminated surface model. Positions of the selected adsorption sites are indicated.

On the Mo-terminated surface, O-Mo distance is shorter on Mo-top site than on two fold (2 fold) and three-coordinated (3 fold) sites. For all the considered sites, the ethanol intermolecular distances are similar to the ones corresponding to the isolated molecule. Only small elongations on C—O and O—H bonds are observed. After adsorption on Mo-terminated surface, there is an increment on C—C—O angle, being the highest for the top site (6%).

On C-terminated surface, considering the adsorption on Mo top site, Mo—O distance and C—C—O angle are higher than the distances on Mo-terminated surface. For the C top and the three-coordinated sites, the ethanol molecule is farther from the surface than in the case of Mo-terminated surface. Besides, the intermolecular distances of the adsorbed species are almost the same as on the isolated molecule.

Table 4 presents the computed charges for the surface and the ethanol molecule before and after adsorption on a Mo top site on the Mo-terminated surface. When ethanol is adsorbed on top on Mo_1 atom, electronic charge of Mo_1 changes from (0.203 *e*) to (0.448 *e*), decreasing its charge by 0.245 *e* (an increase on positive charge means a decrease on electron density, compare columns one and

Table 3
Calculated geometric parameters for isolated ethanol and adsorbed species and adsorption energies (E_{ads}).

		Isolated Ethanol	Ethanol on surface						Ethoxy + H on surface
			Mo Terminated			C Terminated			
			Mo top	2 fold	3 fold	Mo top	C top	3 fold	
E_{ads} (eV)		–	−0.92	−0.83	−0.65	−0.43	−0.17	−0.21	–
Distance (Å)	Mo_{Sup}—O		2.26	2.90	2.86	2.50	–	–	1.91
	C_{Sup}—O		–	–	–	2.80	2.93	4.16	–
	C—O	1.44	1.46	1.46	1.48	1.47	1.44	1.44	1.41
	O—H	0.98	0.98	0.99	0.99	0.98	0.98	0.97	–
	C—C	1.52	1.51	1.51	1.51	1.52	1.52	1.52	1.52
Angle (°)	COH	108.5	111.8	110.8	108.4	108.1	108.8	108.4	–
	CCO	107.1	113.4	108.4	111	115.1	108.7	108.7	112.08

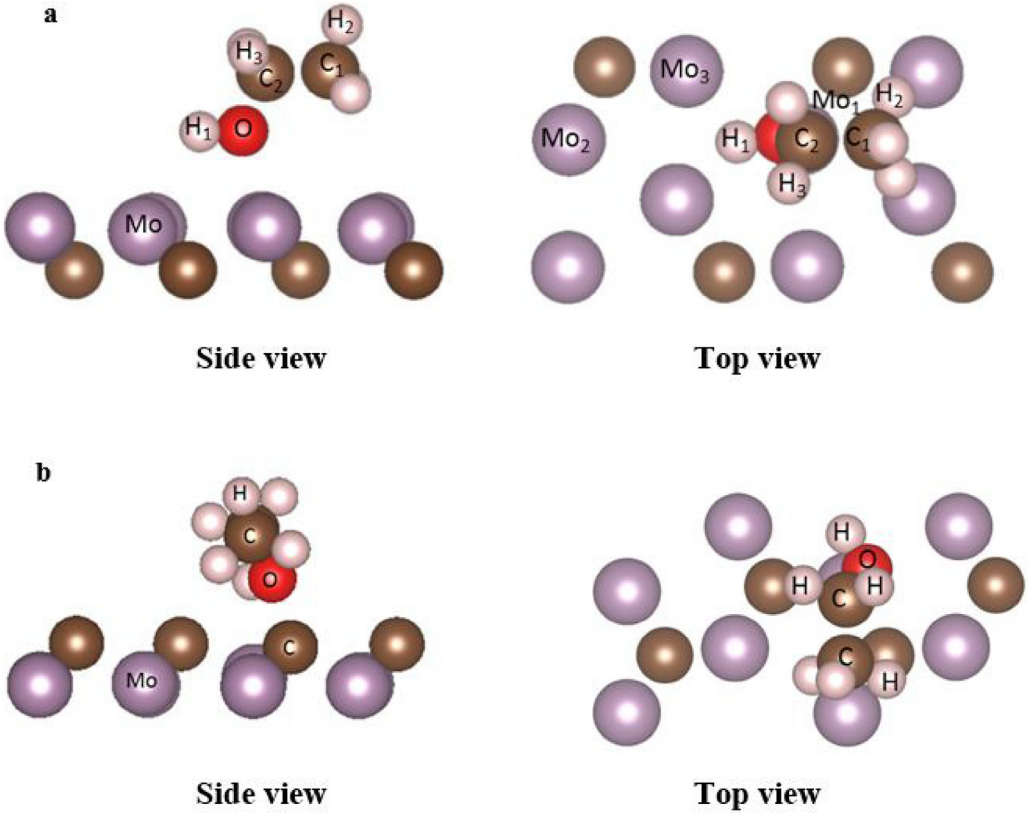

Fig. 5. Surface structure of ethanol adsorbed on a Mo top site on Mo-terminated (a) and C-terminated surfaces (b) (for the sake of clarity, only two surface layers are shown).

Table 4
Net charges for specific atoms on clean Mo-terminated surface of Mo_2C, on isolated and on adsorbed ethanol on Mo_1 top site and after dissociation. C and Mo are labelled in Fig. 5a.

Charge	Isolated		Ethanol on surface	Ethoxy + H
	Surface	Ethanol		
Mo_1	0.203	–	0.448	0.681
Mo_2	0.203	–	0.194	0.355
Mo_3	0.499	–	0.487	0.673
C_1	–	0.080	0.060	0.028
C_2	–	0.662	0.547	0.715
O	–	−1.749	−1.749	−1.294
H_1 (OH)	–	1.000	1.000	−0.485
H_2	–	0.006	0.012	−0.003
H_3	–	−0.005	0.013	0.019
		$q_{ethanol} = 0.00$	$q_{ethanol} = -0.08$	$q_{ethoxy} = -0.52$ $q_H = -0.48$

three of Table 4). More specifically, the charge of the whole surface (considered adding the charge of all the Mo atoms of the first layer of the slab) is reduced by 5%. When the adsorbed species and isolated ethanol are compared, the charge on C atom, near to OH group (C_2), shows an increase of (0.115 *e*). As a result, the total charge of the ethanol molecule becomes (−0.08 *e*). We can then conclude that the surface transfers charge to the molecule, turning it negatively charged.

Fig. 6 shows the plot of the charge density difference for ethanol adsorbed on a Mo top site of the surface. The charge density difference (Δr) isosurface, is calculated using the following equation:

$$\Delta\rho = \rho(\text{ethanol/surface}) - \rho(\text{surface}) - \rho(\text{ethanol})$$

Where " ρ (ethanol/surface)" is the charge density of the ethanol on the surface, "ρ (surface)" is that of the surface after adsorption but without the adsorbate, and "ρ (ethanol)" is that of ethanol in

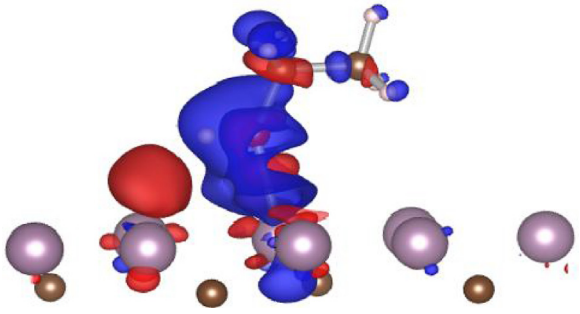

Fig. 6. Charge density difference plots for ethanol adsorbed on $Mo_2C(001)$. Blue color corresponds to charge accumulation (negative) while red color to charge depletion (positive). The isosurface condition is taken as 0.013 e/Å^3. (For interpretation of the references to colour in this figure legend, the reader is referred to the web version of this article.)

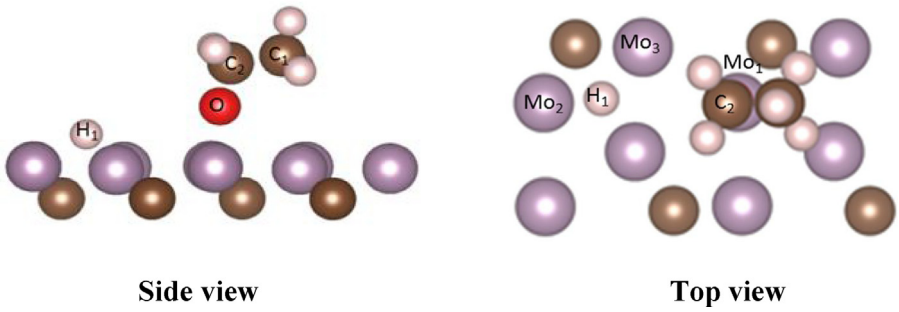

Fig. 7. Surface structure of ethanol dissociation on Mo-terminated Mo_2C surface, side and top views. For clarity, not all the surface is shown and only the first two layers are included.

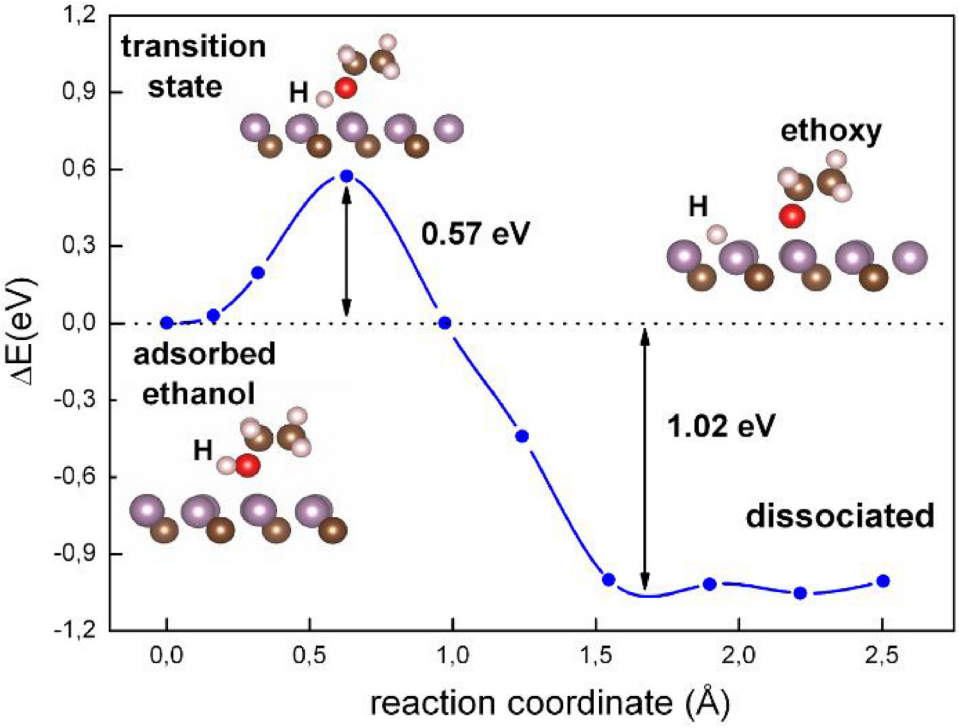

Fig. 8. Reaction coordinate and the corresponding energy variation from adsorbed ethanol to adsorbed ethoxy and H.

the adsorption geometry, but without the substrate. In Fig. 6 it can be seen that more negative charge density accumulation surrounds ethanol (blue colour), while there is some charge depletion on surface Mo atoms close to the adsorbed molecule (red colour), which is consistent with Bader charge analysis.

The ethanol dissociation to ethoxy is a plausible first step for the alcohol decomposition for producing hydrogen, thus this step was analyzed from theoretical approximations. Firstly, ethanol was adsorbed on a top site on Mo-terminated surface. After H abstraction from the OH group, the preferential adsorption sites for the H atom were found by mapping the energy at different locations on surface, while keeping the ethoxy close to its original position, and performing a full geometry optimization of the system (a detailed description of the explored sites is described on Supplementary material section). The three-coordinated sites were the most energetically favourable for H location, as shown in Fig. 7.

The last column of Table 3 shows distances and angle for the ethoxy species. The O—Mo distance was reduced by 0.35 Å when adsorbed and dissociated species are compared; this means that after the dissociation, the ethoxy species are closer to the surface. In addition, C—O distance and the C—C—O angle are also reduced. For the adsorbed H, the average Mo-H distance is 2.04 Å (not indicated in Table 3).

After ethanol dissociation, the charge transfer from the surface is even higher. In this case not only Mo_1 (the closest atom to ethoxy), but also the other Mo atoms close to H, present an important diminution on their charge. Specifically, after dissociation the charge of the whole surface is reduced by 32%. As a result, ethoxy species has a charge of (−0.52 *e*) and the adsorbed H atom results with a charge of (−0.48 *e*).

The pathway connecting the energetically most favourable geometries of adsorbed and dissociated ethanol molecule was examined by CI-NEB calculations. Although several reaction pathways were explored, we only report the most favourable one (other pathways are described on Supplementary material section). Fig. 8 shows the dependence of energy differences on reaction coordinate of the explored pathway, considering the initial step (adsorbed ethanol) as the reference energy level. After the dissociation process, the energy of the system was reduced in −1.02 eV while there is an activation energy barrier of 0.57 eV. A similar energy barrier for methanol dissociation on β-Mo_2C was calculated by DFT by Pistonesi et al. [2]. Studding the conversion of CO_2 into methanol over β-Mo_2C, Posada-Pérez et al. have found that when the methoxy intermediate (H_3CO^*) specie is formed, it is hydrogenated to H_3COH, overcoming an energy barrier of 1.22 eV [34]. A schematic view of the transition state is also included in Fig. 8,

Table 5
Calculated FTIR stretching frequencies of ethanol and its dissociation products.

Vibrational mode	Isolated ethanol frequency (cm^{-1})	Adsorbed ethanol frequency (cm^{-1})	Adsorbed ethoxy + H frequency (cm^{-1})
ν OH	3711	3455	–
ν (CO)	1057	1027	1040
ν(CCO)	863	831	854

which shows an elongation of the OH bond (1.32 Å, 33% longer than on the initial adsorbed state).

Table 5 shows calculated stretching frequencies for the ethanol and ethoxy species. For the ethanol molecule adsorbed on a top site, the stretching frequency for the OH bond is 3455 cm^{-1}, showing a significant shift (256 cm^{-1}) with respect to the frequency of the isolated molecule (3711 cm^{-1}), which could indicate a possible activation of the bond.

CO stretching frequency shows a small decrease with respect to the value for the isolated molecule. These results are in agreement with small elongation of OH and CO bonds. Similar results have been found for stretching frequencies of the methanol adsorbed on molybdenum carbides [18].

After dissociation there is a small increase of the stretching frequencies for the CO bond, according to the shortening of this bond.

4. Conclusions

A β-Mo_2C sample was prepared from the reduction of a mixture of molybdenum salts and char. The catalyst presents a specific surface area of 34 m^2/g and it is quite stable to thermal treatment. The desorption of H_2, following ethanol adsorption was detected over this catalyst at 500–600 K.

According to DFT calculations, ethanol would adsorb more strongly on Mo-terminated surfaces than on C-terminated ones, with an adsorption energy of −0.92 eV. The role of the molybdenum carbide surface would be to transfer electron density to the adsorbed ethanol molecule, making it negatively charged. Dissociation of ethanol to ethoxy species is energetically favorable, in agreement with our experimental results. CI-NEB calculations for the activation energy of ethanol dissociation over Mo_2C surface throw a value of 0.57 eV. The computed shift of the stretching frequency of the OH bond after ethanol adsorption is in agreement with the idea of the activation of the bond to produce dissociation to ethoxy species.

Acknowledgments

The authors are grateful for the financial support from MINCyT-MEYS ARC/13/11, SGCyT-UNS PGI 24/F128 and PICT 2014-1351. C.P and M.E.P. are members of CONICET.

Appendix A. Supplementary data

Supplementary data associated with this article can be found, in the online version, at http://dx.doi.org/10.1016/j.mcat.2017.07.003.

References

[1] J.G. Chen, Carbide and nitride overlayers on early transition metal surfaces: preparation, characterization, and reactivities, Chem. Rev. 96 (1996) 1477–1498.
[2] C. Pistonesi, A. Juan, A.P. Farkas, F. Solymosi, DFT study of methanol adsorption and dissociation on β-Mo_2C (001), Surf. Sci. 602 (2008) 2206–2211.
[3] A.P. Fakas, F. Solymosi, Effects of potassium on the adsorption and dissociation pathways of methanol and ethanol on Mo_2C/Mo(100), Surf. Sci. 602 (2008) 1475–1485.
[4] R.B. Levy, M. Boudart, Platinum-like behavior of tungsten carbide in surface catalysis, Science 181 (1973) 547–549.
[5] J. Raskó, M. Dömök, K. Baán, A. Erdöhelyi, FTIR and mass spectrometric study of the interaction of ethanol and ethanol–water with oxide-supported platinum catalysts, Appl. Catal. A: Gen. 299 (2006) 202–211.
[6] S.-K. Xing, G.-C. Wang, Reaction mechanism of ethanol decomposition on Mo_2C (100) investigated by the first principles study, J. Catal. 377 (2013) 180–189.
[7] R. Barthos, A. Széchenyi, F. Solymosi, Efficient H_2 production from ethanol over Mo_2C/C nanotube catalyst, Catal. Lett. 120 (2008) 161–165.
[8] R. Barthos, F. Solymosi, Hydrogen production in the decomposition and steam reforming of methanol on Mo_2C/carbon catalysts, J. Catal. 249 (2007) 289–299.
[9] (a) R. Barthos, A. Széchenyi, Á. Koós, F. Solymosi, The decomposition of ethanol over Mo_2C/carbon catalysis, Appl. Catal. A: Gen. 327 (2007) 95–105; (b) A. Széchenyi, F. Solymosi, Production of hydrogen in the decomposition of ethanol and over unsupported Mo_2C catalysts, J. Phys. Chem. C 111 (2007) 9509–9515.
[10] W. Ding, S. Li, G. Meitzner, E. Iglesias, Phys. Chem. B 105 (2) (2001) 506–513.
[11] J. Ren, C. Huo, J. Wang, Y. Li, H. Jiao, Surface structure and energetics of oxygen and CO adsorption on α-Mo_2C(0001), Surf. Sci. 596 (2005) 212–221.
[12] J. Ren, C. Huo, J. Wang, Z. Cao, Y. Li, H. Jiao, Density functional theory study into the adsorption of CO_2,H and CH_x (x = 0–3) as well as C_2H_4 on α -Mo_2C(0 0 0 1), Surf. Sci. 600 (2006) 2329–2337.
[13] H. Tominaga, M. Nagai, Density functional theory of water-gas shift reaction on molybdenum carbide, J. Phys. Chem. B 109 (2005) 20415–20423.
[14] H. Tominaga, M. Nagai, Theoretical study of methane reforming on molybdenum carbide, App. Catal. A: Gen. 328 (2007) 35–42.
[15] C. Pistonesi, M.E. Pronsato, L. Bugyi, A. Juan, The adsorption of CO on potassium doped molybdenum carbide surface: an ab-initio study, Catal. Today 181 (2012) 102–107.
[16] C. Pistonesi, M.E. Pronsato, L. Bugyi, A. Juan, Theoretical model for CO adsorption and dissociation on clean and K-doped β-Mo_2C surfaces, J. Phys. Chem. C 116 (2012) 24573–24581.
[17] M.E. Pronsato, C. Pistonesi, A. Juan, A.P. Farkas, L. Bugyi, F. Solymosi, Density Functional Theory study of methyl iodide adsorption and dissociation on clean and K-promoted β -Mo_2C surfaces, J. Phys. Chem. C 115 (2011) 2798–2804, American Chemical Society, USA.
[18] C. Pistonesi, A. Juan, A.P. Farkas, F. Solymosi, Effects of potassium on the adsorption of methanol on β-Mo_2C(001) surface, Surf. Sci. 604 (2010) 914–919, Elsevier, USA.
[19] http://cms.mpi.univie.ac.at/vasp/vasp/vasp.html.
[20] G. Kresse, J. Furthmüller, Efficiency of ab-initio total energy calculations for metals and semiconductors using a plane-wave basis set, J. Comput. Mater. Sci. 6 (1996) 15–50.
[21] G. Kresse, Furthmüller, Efficient iterative schemes for ab initio total-energy calculations using a plane-wave basis set, J. Phys. Rev. B 54 (1996) 11169–11186.
[22] G. Kresse, D. Joubert, From ultrasoft pseudopotentials to the projector augmented-wave method, Phys. Rev. B 59 (1999) 1758–1775.
[23] J.P. Perdew, K. Burke, M. Ernzerhof, Generalized gradient approximation made simple, Phys. Rev. Lett. 77 (1996) 3865–3868.
[24] J.P. Perdew, K. Burke, M. Ernzerhof, Generalized gradient approximation made simple [Phys. Rev. Lett. 77, 3865 (1996)], Phys. Rev. Lett. 78 (1997), 1396-1396.
[25] W.H. Press, B.P. Flannery, S.A. Teukolsky, W. Vetterling, Numerical Recipies, Cambridge University Press, New York, 1986, pp. 301.
[26] S. Grimme, Semiempirical GGA-type density functional constructed with a long-range dispersion correction, J. Comput. Chem. 27 (2006) 1787.
[27] H. Jonson, G. Mills, K. Jacobsen, Nudged elastic band method for finding minimum energy paths of transitions, in: Berne, Ciccotti, Coker (Eds.), Classical and Quantum Dynamics in Condensed Phase Simulations, World Scientific, River Edge, NJ, 1998, p. 385.
[28] G. Henkelman, B. Uberuaga, H.A. Jónsson, A climbing image nudged elastic band method for finding saddle points and minimum energy paths, J. Chem. Phys. 113 (2000) 9901.
[29] W. Tang, E. Sanville, G. Henkelman, A grid-based Bader analysis algorithm without lattice bias, J. Phys.: Condens. Matter 21 (2009) 84204–84210.
[30] E. Parthé, V. Sadagopan, The structure of dimolybdenum carbide by neutron diffraction technique, Acta Crystallogr. 16 (1963) 202–205.
[31] (a) J.T. Kummer, J. Phys. Chem. 90 (1986) 4747;
(b) B.H.S. Gandhi, H.C. Yao, H.K. Stepien, Catalysis Under Transient Conditions, in: A.T. Bell, L. Hegedus (Eds.), ACS Symposium Series No. 178, American Chemical Society, 1982, p. 143;
(c) I. Halasz, A. Brennef, Appl. Catal. A: Gen. 82 (1992) 51–63.
[32] L.L. Seigle, C.L. Chang, T.P. Sharma, Free energy of formation of Mo_2C and the thermodynamic properties of carbon in solid molybdenum, Metall. Trans. A 10 (1979) 1223–1228.
[33] A. Farkas, F. Solymosi, Adsorption and reactions of ethanol on Mo_2C/Mo(100), Surf. Sci. 601 (2007) 193–200.
[34] S. Posada-Pérez, P.J. Ramírez, R.A. Gutiérez, D.J. Stacchiola, F. Viñas, P. Liu, F. Illasa, J.A. Rodriguez, The conversion of CO_2 to methanol on orthorhombic β-Mo_2C and Cu/β-Mo_2C catalysts: mechanism for admetal induced change in the selectivity and activity, Catal. Sci. Technol. (2016) 6766–6777.